Journal of Molecular Catalysis A: Chemical 304 (2009) 52–57

Contents lists available at ScienceDirect

Journal of Molecular Catalysis A: Chemical

journal homepage: www.elsevier.com/locate/molcata

Synthesis and characterization of mesoporous phosphotungstic acid/TiO_2 nanocomposite as a novel oxidative desulfurization catalyst

Xue-Min Yan[a,*], Ping Mei[a], Jiaheng Lei[b], Yuanzhu Mi[a], Lin Xiong[a], Liping Guo[b]

[a] College of Chemistry and Environmental Engineering, Yangtze University, Nanhuan Road No. 1, Jingzhou 434023, PR China
[b] Department of Applied Chemistry, Wuhan University of Technology, Wuhan 430070, PR China

ARTICLE INFO

Article history:
Received 14 November 2008
Received in revised form 14 January 2009
Accepted 14 January 2009
Available online 21 January 2009

Keywords:
Oxidative desulfurization
Refractory sulfur compounds
Dibenzothiophene
Mesoporous HPW/TiO_2
Selectivity

ABSTRACT

A series of mesoporous phosphotungstic acid/TiO_2 (HPW/TiO_2) nanocomposites with various HPW contents have been synthesized by evaporation-induced self-assembly method. These nanocomposites were used as catalysts for oxidative desulfurization of model fuel, which was composed of dibenzothiophene (DBT) and hydrocarbon, and used H_2O_2 as oxidant. These catalysts were characterized by X-ray diffraction (XRD), nitrogen adsorption–desorption isotherm, transmission electron microscopy (TEM), FTIR and UV–vis. Characterization results suggest that these mesoporous HPW/TiO_2 possessed relatively uniform channel-like pores with Barrett–Joyner–Halenda (BJH) pore size of about 4 nm. The Brunauer–Emmett–Teller (BET) surface of the mesoporous HPW/TiO_2 slightly increases with the increase of HPW content and reach to a peak value of 176 m^2/g and 0.25 cm^3/g when the HPW content is 30 wt%. Keggin-type heteropolyacids (HPAs) has been encapsulated into anatase TiO_2 framework and the average size of TiO_2 nanoparticles is 8 nm. Catalytic oxidation results show that the catalysts are very active in refractory bulky molecule organosulfur compounds in fuel oil. The oxidative removal of DBT increases as the HPW content increases. The mesoporous HPW/TiO_2 also shows high selectivity for DBT oxidation in the DBT–petroleum ether–benzene system. The selective desulfurization ratio reach to 95.2% with mesoporous HPW/TiO_2 (20 wt%) catalyst under the reaction condition of 333 K, 2 h. In addition, the mesoporous HPW/TiO_2 catalyst shows excellent reusing ability, which makes it a promising catalyst in oxidative desulfurization process.

1. Introduction

Deep desulfurization of transportation fuels has become an important research subject due to the increasingly stringent regulations and fuel specifications in many countries for environmental protection purpose [1]. Conventional hydrodesulfurization (HDS) process is difficult to remove alkylsubstituted dibenzothiophenes like 4,6-dimethyldibenzothiophene, which are refractive to HDS due to steric hindrance. In order to produce ultralow sulfur diesel fuel with HDS process, higher temperature, higher pressure, larger reactor volume, and more active catalysts are required [2]. In addition, the severe conditions lead to negative effects, such as the decrease of catalyst life, higher hydrogen consumption, and higher yield losses resulting in higher costs. Therefore, alternative desulfurization techniques have been investigated widely, among which oxidative desulfurization (ODS) is considered to be one of the promising new methods for super deep desulfurization of fuel oil [3]. In the ODS process, the refractory dibenzothiophene (DBT) and 4,6-dimethydibenzothiophene (4,6-DMDBT) are oxidized to their corresponding sulfones under mild conditions, which are subsequently removed by extraction, adsorption, distillation, or decomposition [4–8].

Various oxidants have been used in ODS, such as NO_2 [9], O_3 [10], H_2O_2 [2], *tert*-butyl hydroperoxide [11], molecular oxygen [12], K_2FeO_4 [13] and solid oxidizing agents [14]. Among these oxidants, H_2O_2 is mostly chosen as an oxidant, only producing water as a byproduct. Peracids produced in situ from organic acids catalysts and H_2O_2 are reported to be very effective for rapid oxidation of sulfur compounds in fuel oils under mild conditions. Heteropolyacid catalysts in H_2O_2 oxidation system have also exhibited high catalytic activity for the oxidation of BTs and DBTs [2,15,16]. However, the main obstacles for these catalysts to the industrial application of the process at present are the difficulties in separation and recovery. Therefore, the use of solid catalysts in ODS processes has been developed in recent years. Many types of solid catalysts have been attempted, such as Ti molecular sieves [17,18], WOx/ZrO_2 [19] and vanadium oxide [20]. However, the selectivity of these catalysts for sulfides in fuels is not high, and some components of the fuel are also oxidized. Therefore, the solid catalysts with high selectivity is highly desirable in heterogeneous ODS system.

* Corresponding author. Tel.: +86 716 8488 998; fax: +86 716 8060 650.
E-mail address: yanzhangmm2002@163.com (X.-M. Yan).

1381-1169/$ – see front matter © 2009 Elsevier B.V. All rights reserved.
doi:10.1016/j.molcata.2009.01.023

In the current research, an efficient heterogeneous ODS catalyst mesoporous HPW/TiO_2 nanocomposite was obtained by incorporating tungstophosphoric acid into mesoporous titania with evaporation-induced self-assembly method. The nanocomposites were characterized by various analytical and spectroscopic techniques such as X-ray diffraction (XRD), nitrogen adsorption–desorption isotherm, transmission electron microscopy (TEM), FTIR and UV–vis. The catalytic activity and selectivity of the catalysts were systematically evaluated in the desulfurization of model fuel.

2. Experimental

2.1. Synthesis of mesoporous HPW/TiO_2

The mesoporous HPW/TiO_2 was prepared by using $EO_{20}PO_{70}EO_{20}$ (Pluronic P123, Sigma) as a structure-directing agent, and using tetrabutyl titanate ($Ti(C_4H_9O)_4$, Sigma–Aldrich) as the titania precursor. In a typical synthesis, 3.40 g $Ti(C_4H_9O)_4$ and 2.40 g acetic acid were dissolved in 20 mL ethanol with stirring, and then an amount of 12-phosphotungstic acid was added slowly. The mixture was adjusted to pH 1–2 by adding hydrochloric acid (HCl, 36%) to form sol A. 1.20 g P123 was dissolved in 15 mL ethanol to prepare solution B. After the sol A was magnetically stirred for about 2 h at room temperature, the solution B was filled slowly and magnetically stirred for another 2 h. The resulting sol solution with molar composition 1 $Ti(C_4H_9O)_4$:0.02 P123:4HOAc:60 C_2H_5OH:*x*HPW was poured into Petri dish and maintained for 2 days at 313 K and then was transferred into a 333 K oven and aged for another 2 days. As-synthesized mesostructured composites were calcined at 673 K in air for 10 h (ramp rate 1 °C/min) to obtain mesoporous HPW/TiO_2 with 10–40 wt% HPW concentration.

2.2. Characterization of the catalysts

The obtained mesoporous HPW/TiO_2 samples were first ground into fine powder for characterization. XRD patterns were recorded on a Rigaku D/MAX-RB diffractometer with a Cu Kα radiation operating at 40 kV, 50 mA. TEM images were taken with a FEI TECNAI G2 20 electron microscope operating at 200 kV. The TEM samples were prepared by dispersing the particles in alcohol, which then were deposited onto a Cu grid and left drying in air. Nitrogen adsorption–desorption data were measured with a Quantachrome Autosorb-1 analyzer at 77 K. The samples were outgassed at 473 K for 6 h prior to the measurements. The surface area was calculated by the Brunauer–Emmett–Teller (BET) method. The pore size distribution was derived from the adsorption branches of the isotherms using the Barrett–Joyner–Halenda (BJH) method. FTIR spectra (1400–600 cm^{-1}) were recorded on a Digilab-FTS60 spectrometer. The samples were pressed with KBr in the ratio 1:150. Diffuse reflectance UV–vis spectra were measured with a spectrometer of PE Lambda 35 equipped with the integrating sphere using $BaSO_4$ as the reference. The HPW content in solid samples was determined by the results of inductively coupled plasma analysis (ICP, Perkin-Elmer 3300DV).

2.3. Desulfurization of model fuel

The experiments of oxidative desulfurization were performed in a 150 mL flask equipped with stirrer and condenser. Two kinds of model fuels with sulfur content of 500 μg/g were obtained by dissolving DBT in petroleum ether, and petroleum ether + benzene (with volume ratio of 3:1), respectively. In the typical run, the water bath was first heated and stabilized to a certain temperature. 0.2 g of catalyst was added to a mixture of 20 mL of model fuels and 20 mL of acetonitrile. Then a certain amount of 30% aqueous H_2O_2 was added to start the reaction. The amount of oxidant was expressed as O/S mole ratio. The resulting mixture was stirred for 2 h at the reaction temperature and analyzed periodically. The catalyst was centrifuged off, the oil phase and solvent phase were respectively analyzed by WK-2C total sulfur analyzer and a gas chromatograph equipped with a pulsed flame photometric detector (PFPD, agilent-6890, capillary column HP-5). The catalyst was washed with toluene for several times, heated at 573 K for 4 h and reused in the next run.

3. Results and discussion

3.1. XRD patterns

Fig. 1 shows small-angle and wide-angle powder XRD patterns of mesoporous HPW/TiO_2 samples with different HPW contents. As is observed in Fig. 1A, the samples with HPW content of 10–30 wt% present well-resolved diffraction peak at $2\theta = 1–3°$ typical for mesostructured materials [21]. Only one XRD peak in the low angle range indicates that no long-range order pore arrangement exists in our samples. When HPW content in the HPW/TiO_2 composite increased to 40 wt%, significant shrinkage of the diffraction peak of above 50% is observed. At the same time, the diffractions slightly shift to the high angles, suggesting the destruction of the ordered mesostructure. The wide-angle XRD patterns of the

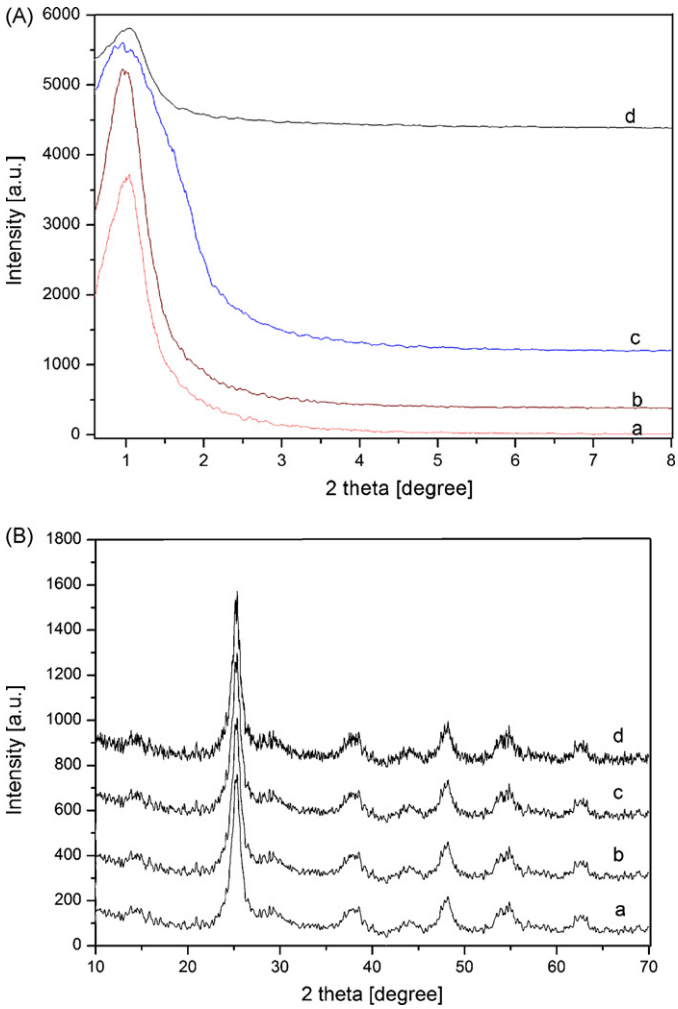

Fig. 1. Small-angle (A) and wide-angle (B) XRD patterns of mesoporous HPW/TiO_2 samples: (a) 10 wt%, (b) 20 wt%, (c) 30 wt% and (d) 40 wt%.

Table 1
The HPW content and structural parameters of different catalysts.

Samples	HPW content		Pore size (nm)	S_{BET} (m^2/g)	Pore volume (cm^3/g)
	Gel (wt%)	Product (wt%)			
HPW/TiO_2 (10 wt%)	10	9.5	3.6	170	0.19
HPW/TiO_2 (20 wt%)	20	19.2	3.6	175	0.21
HPW/TiO_2 (30 wt%)	30	28.1	3.9	176	0.25

mesoporous HPW/TiO_2 are presented in Fig. 1B. The characteristic peaks of anatase appeared in this wide-angle XRD patterns, suggesting the existence of nanocrystalline anatase in mesostructure framework of composite. As calculated from the Scherrer equation using the (1 0 1) diffraction peak of anatase, the average crystallite size is found to be 8 nm. No evident peak for HPW crystalline phases is found on wide-angle XRD patterns of these samples, which indicates that HPW clusters are successfully dispersed in the mesoporous anatase TiO_2 framework rather than existing in free solid acid. The HPW contents of mesoporous HPW/TiO_2 samples in the final products detected by ICP are listed in Table 1. The determined loadings of HPW are close to the expected values, indicating that the losses of HPW are insignificant in our prepared process.

3.2. TEM images

The mesoporous structure and the nature of channel walls of the mesoporous HPW/TiO_2 were characterized by TEM and HRTEM. Fig. 2A is the TEM image of mesoporous HPW/TiO_2 with 20 wt% HPW content. No mesostructure with long-range order can be observed in the TEM images, which is consistent with the low-angle XRD results. Furthermore, the corresponding HRTEM image of the sample (Fig. 2B) evidenced the presence of many anatase nanocrystalline particles, indicating that these nanocrystalline particles are connected with each other to form a crystalline framework. The particles size of the TiO_2 nanoparticles is approximately 8 nm, which is consistent with the crystallite size estimated from XRD analysis.

3.3. N_2 adsorption isotherms

Fig. 3A shows the N_2 adsorption isotherms of the mesoporous HPW/TiO_2 samples with various HPW contents. All samples display type IV isotherms with H2 hysteresis loops, which are related to the mesoporous structure. H2 hysteresis loops are observed for materials with relatively uniform channel-like pores, when the desorption branch happens to be located at relative pressure around $P/P_0 = 0.4$ [22]. BJH pore size distribution plots are shown in Fig. 3B. The samples exhibited uniform pore size distributions with the mean pore size of about 4 nm. The BET surface area and pore volume of the mesoporous HPW/TiO_2 samples are summarized in Table 1. The BET surface area and pore volume of 10 wt% HPW content sample are 170 m^2/g and 0.19 cm^3/g; the corresponding values of 20 wt% and 30 wt% HPW content samples are 175 m^2/g and 0.21 cm^3/g, and 176 m^2/g and 0.25 cm^3/g, respectively. The BET surface area and pore volume were mainly influenced by the growth of TiO_2 particles. As for the mesoporous HPW/TiO_2 samples, the anchoring of HPW in mesoporous framework restrains efficiently the growth of TiO_2 particles [23]. Therefore, the BET surface area and pore volume slightly enhance with the increase of HPW content in composite. Nevertheless, further increase of HPW content to 40 wt%, the hydrolysis of tetrabutyl titanate becomes so accelerated [24]. As a result, the high polymeric Ti–HPW entities are formed, which are relatively difficult to assemble with the template, and therefore result in degradation of the mesostructure.

3.4. FTIR spectra and UV–vis

FT-IR spectra of HPW and mesoporous HPW/TiO_2 samples are shown in Fig. 4. It has been widely reported that HPW with Keggin structures gives several strong, typical IR bands at ca. 1079 cm^{-1} (stretching frequency of P–O in the central PO_4 tetrahedron), 983 cm^{-1} (terminal bands for W=O in the exterior WO_6 octahedron), 889 cm^{-1} and 805 cm^{-1} (bands for the W–O_b–W and W–O_c–W bridge, respectively) [25,26]. The peaks of mesoporous HPW/TiO_2 samples appearing in the range from 1100 cm^{-1} to 700 cm^{-1} are ascribed to the stretch vibrations of P–O, W=O, and W–O–W bonds of the Keggin units, respectively, indicating that the primary Keggin structures of these polyoxotungstates remain intact

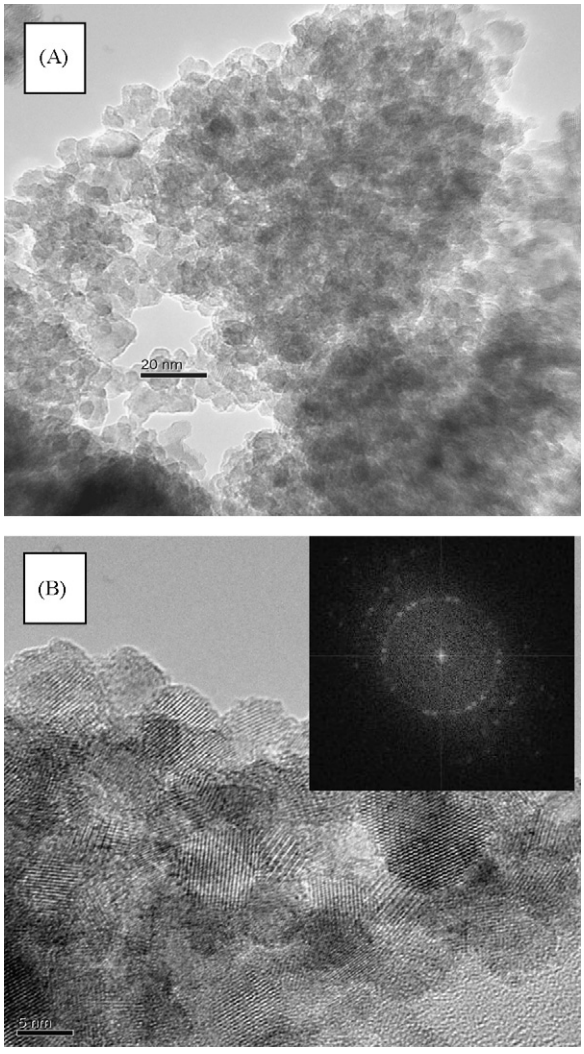

Fig. 2. TEM (A) and HRTEM (B) images of mesoporous HPW/TiO_2 sample with 20 wt% HPW content. The inset in part (B) is the modulus of the Fourier transform of the full image.

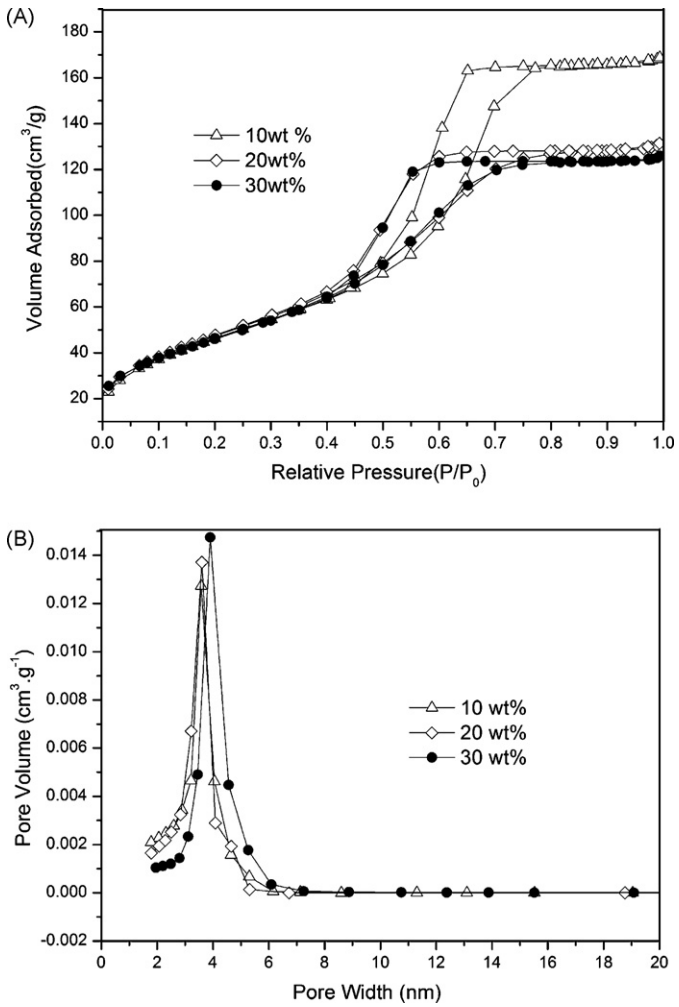

Fig. 3. Nitrogen adsorption/desorption isotherm (A) and BJH pore size distribution plots (B) of mesoporous HPW/TiO2 samples.

after the formation of the composites. UV–vis/DRS of the parent HPW, as-prepared TiO_2, and mesoporous HPW/TiO_2 are shown in Fig. 5. Bulk HPW shows the absorption bands at 260 nm and 320 nm, which agrees well with the literature data [27]. As for the TiO_2, the

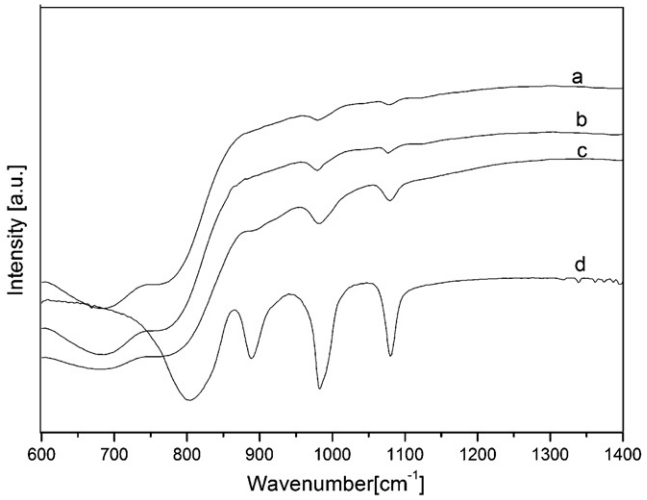

Fig. 4. IR spectra of various samples: (a) HPW/TiO_2 (10 wt%), (b) HPW/TiO_2 (20 wt%), (c) HPW/TiO_2 (30 wt%) and (d) HPW.

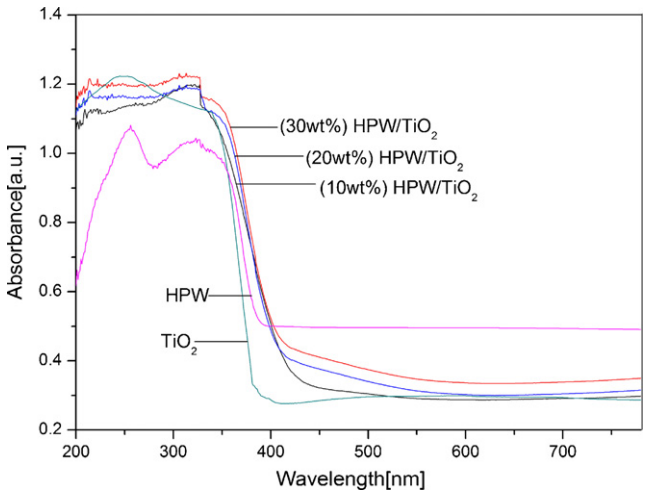

Fig. 5. UV–vis spectra of various samples.

absorption maximum is at 245 nm, corresponding to CT from O 2p to Ti 3d of anatase TiO_2 [28]. The HPW/TiO_2 crystallites exhibited broad and strong absorption in the range from 200 nm to 400 nm, which is different from the original HPW and anatase TiO_2. The red shifts are observed compared with the parent HPW and TiO_2. The above UV–vis/DRS results indicate that the introduction of HPW into TiO_2 framework has an influence on coordination environment of TiO_2 crystalline, resulting in the red shifts of the absorption band [29–31].

3.5. Desulfurization over mesoporous HPW/TiO_2

Fig. 6 shows the DBT conversion versus reaction temperature with catalysts of different HPW concentrations while the O/S molar ratio is 12. As for the catalysts with identical composition, the higher the temperature is, the higher the desulfurization rate is. The mesoporous HPW/TiO_2 with 20 wt% HPW content gives the DBT conversions of 70.0% at 303 K and the corresponding conversions close to 100% at 353 K. In addition, higher DBT conversion can be obtained with the increase of HPW concentrations in mesoporous HPW/TiO_2.

The oxidation reaction of DBT was also carried out under various O/S molar ratios at 333 K with mesoporous HPW/TiO_2 (20 wt%) as the catalyst in order to investigate the effect of the amount of the oxidant on the oxidation activity. As is shown in Fig. 7, the oxidation

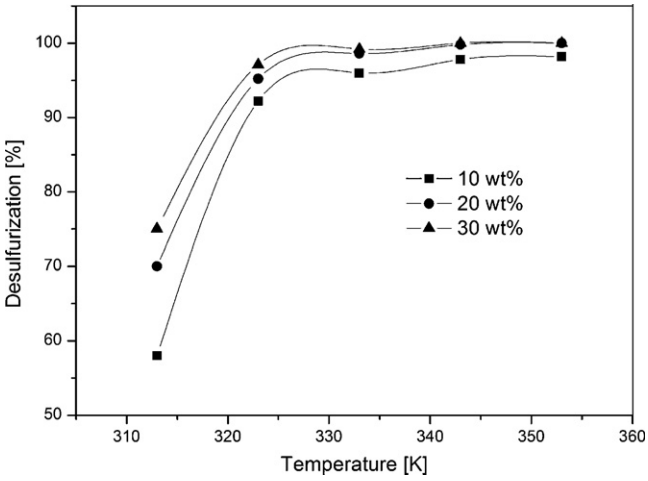

Fig. 6. Desulfurization abilities of mesoporous HPW/TiO_2 at various temperatures.

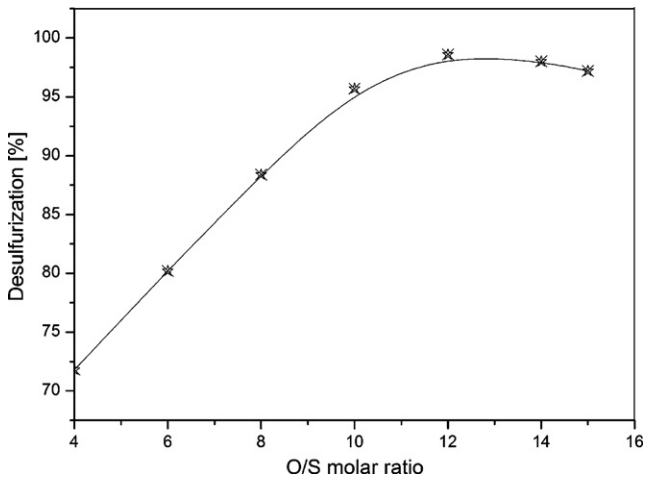

Fig. 7. Conversion of DBT under various O/S molar ratio at 333 K with mesoporous HPW/TiO_2 (20 wt%) as catalyst.

activity of DBT increase with the O/S molar ratio up to O/S = 12 and then slightly decrease beyond this value. This optimal value of O/S molar ratio is much higher than the value of stoichiometric O/S molar ratio which is needed to oxidize DBT. The excess of oxidant can be attributed to the side reactions involving the thermal decomposition of hydrogen peroxide. These results show the balance of two opposing factors, i.e., the excess of oxidant increases the activity while the water produced from ODS reaction and thermal decomposition hinders the ODS reaction [32]. Hence, it is very important to control the oxidant addition in these reactions.

The competitive reactions of a mixture of BT, DBT and 4,6-DMDBT was also carried out. The total sulfur content of the mixture is 500 μg/g. Fig. 8 shows that the oxidative reactivity of the model sulfur compounds follows the order of DBT > 4,6-DMDBT > BT. After 2-h reaction, using mesoporous HPW/TiO_2 (20 wt%) as catalyst at 333 K, DBT conversion is almost 100% while 4,6-DMDBT conversion approaches 97.8% and the BT conversion only reaches 94.6%. The observed order of reactivity is different from what is observed in the HDS process where the most sterically hindered 4,6-DMDBT is the least reactive. Apparently, both the electron density on the sulfur atom and the steric hindrance of the methyl groups govern the reactivity. Comparing to other sulfur compounds, BT exhibits the lowest reactivity due to the significantly lower electron density on its sulfur atom. For DBT and 4,6-DMDBT, the difference in

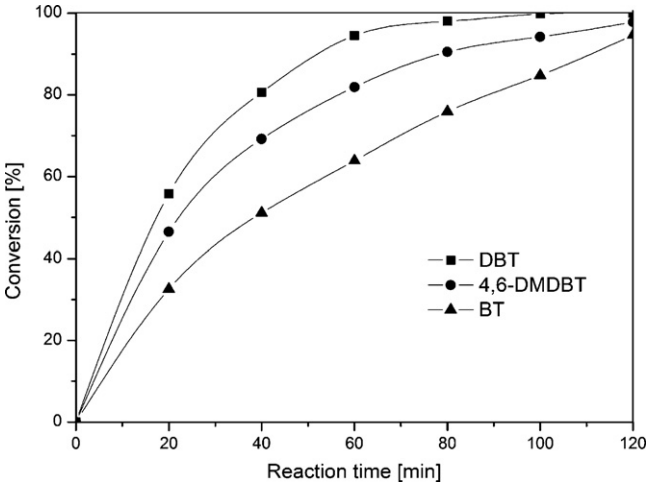

Fig. 8. Conversion of different organic sulfur compounds as functions of reaction times at 333 K with mesoporous HPW/TiO_2 (20 wt%) as catalyst.

the electron density on the sulfur is very small (5.758 versus 5.760) [33], and it is the steric hindrance of the methyl groups that governs the reactivity. The methyl groups become an obstacle for the sulfur atom to approach the catalytically active site in a heterogeneous system. It is in good agreement with the results of Ishihara et al. [33] who has performed the oxidation of sulfur compounds by t-BuOOH with Mo/Al_2O_3 as the catalyst.

Although the mesoporous HPW/TiO_2 has shown efficient catalytic activity in the DBT–petroleum ether system, the selectivity of the mesoporous HPW/TiO_2 for sulfides should be investigated by the reason that some components of the fuel, such as alkenes and aromatic hydrocarbons, can also be oxidized. The selective desulfurization capacity of mesoporous HPW/TiO_2 was carried out in the DBT–petroleum ether–benzene system. As a comparison, the desulfurization capacity of other catalysts, including mesoporous HPW/SiO_2 with identical HPW content [34] and the HPW/TiO_2 without mesoporous structure prepared from the sol–gel derived route, are also researched. The experiment results are shown in Table 2, which indicate that mesoporous HPW/TiO_2 has the highest desulfurization rate among the catalysts involved in this paper at low temperature and atmospheric pressure. The higher desulfurization rate in experiment 1 than that in experiment 2 can be attributed to the big pore size of mesoporous HPW/TiO_2. DBT is a relatively large molecule with molecular dynamics diameter of 1.7 nm. The pore size of mesoporous HPW/TiO_2 is much larger than 1.7 nm, thus diffusion resistance of the catalytic oxidation is reduced. Compared with experiment 3, the higher desulfurization rate in experiment 1 can be attributed to the surface properties of catalysts. It is well known that TiO_2 is Lewis acidity oxide. Therefore, the mesoporous HPW/TiO_2 has higher Lewis acidity than mesoporous HPW/SiO_2 due to the coordinately unsaturated Ti^{4+} species on mesoporous HPW/TiO_2 [35]. The DBT series compounds can display some Lewis basic character due to the available free lone electron pairs of these compounds. DBT is more basic than benzene, hence, the sulfur compounds can be preferentially adsorbed on mesoporous HPW/TiO_2 surface according to a Lewis-type acid–base interaction. The adsorption of DBT on the catalyst surface can increase the collision probability of DBT and the catalytic active sites, which will accelerate the oxidation reaction. The selective adsorption capacities of different catalysts for DBT in petroleum ether–benzene system were carried out and the results were also summarized in Table 2. The mesoporous HPW/TiO_2 shows evidently higher adsorption capacity than that of mesoporous HPW/SiO_2. Therefore, the selective oxidation process can be supposed to be that the existence of Lewis acidity sites is responsible for the selective adsorption of the DBT, and then the DBT is oxidized at the HPW sites. The resultant products desorb from the catalyst surface and enter into the polar solvent, which allows the active sites to be recovered for further reaction.

The polar solvent plays a very important role in the catalytic reactions carried out in the liquid phase. Sulfur compounds are known to be slightly more polar than hydrocarbons with similar structures. Oxidized sulfur compounds, such as sulfones and sulfoxides are substantially more polar than corresponding sulfides. During ODS process the products are transferred to the polar solvent, and the solvent can influence the mass transport and diffusional problems, especially with porous catalysts [32]. In addition, in order to study the solvent effect on the ODS of model fuel, we have monitored the solvent phase in the reaction process. The experiment results are shown in Table 2. A fraction of DBT removed from oil phase was not transformed to its corresponding sulfone, under these experimental conditions. They are only removed as sulfur compounds through extraction, without ODS reaction.

The reusing ability of mesoporous HPW/TiO_2 in the desulfurization process has also been investigated. The desulfurization experiments were carried out in DBT–petroleum ether system with

Table 2
Comparison experiments.

Serial number	Catalyst	Oxidant	DBT content (μg/g)			Total desulfurization rate (%)
			Feed	Solvent phase	Oil phase	
1	Meso-HPW/TiO_2[a]	H_2O_2	500	51	24	95.2
2	HPW/TiO_2[b]	H_2O_2	500	70	198	60.4
3	Meso-HPW/SiO_2[c]	H_2O_2	500	62	75	85.0
4	Meso-HPW/TiO_2	–	500	76	348	30.4
5	Meso-HPW/SiO_2	–	500	78	401	19.8

Operating parameters—reaction time: 2 h; reaction temperature: 333 K; O/S: 12; catalysts amount: 0.2 g.
[a] Meso-HPW/TiO_2: mesoporous HPW/TiO_2 with 20 wt% HPW content.
[b] HPW/TiO_2: HPW/TiO_2 without mesoporous structure prepared from the sol–gel derived route.
[c] Meso-HPW/SiO_2: mesoporous HPW/SiO_2 with 20 wt% HPW content prepared by the literature [34] method.

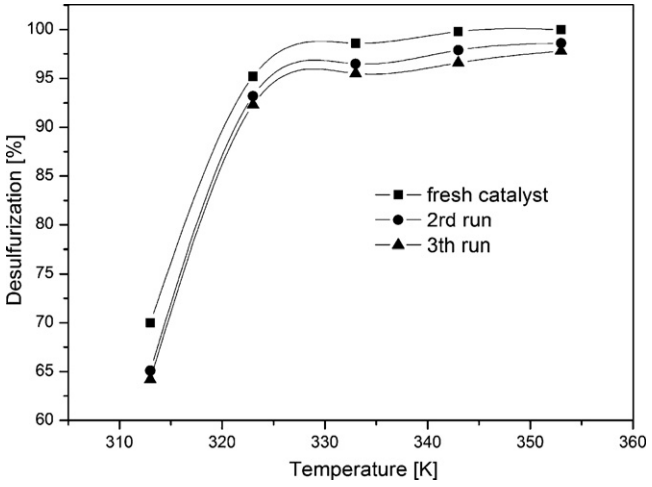

Fig. 9. The reusing ability of mesoporous HPW/TiO_2 (20 wt%).

mesoporous HPW/TiO_2 (20 wt%) as catalyst and the results are shown in Fig. 9. It can be seen that after three times of regeneration, the desulfurization rate of mesoporous HPW/TiO_2 is only slightly lower than the fresh catalyst. The excellent reusing ability can be attributed to the chemical interactions between the HPW and TiO_2 framework, which can prevent HPW from leaching in polar solution. In addition, oxidation products adsorbed on mesoporous HPW/TiO_2 can be removed at 573 K, and at this temperature HPW and the molecular sieve are both stable [36], therefore the mesoporous HPW/TiO_2 may easily restore the catalytic activity.

4. Conclusions

In conclusion, we have successfully prepared the mesoporous HPW/TiO_2 nanocomposites with HPW content of 9.5–28.1 wt% by evaporation-induced self-assembly method. HPW clusters are successfully dispersed in the mesoporous anatase TiO_2 framework and the average size of the TiO_2 nanoparticles is approximately 8 nm. The mesoporous HPW/TiO_2 nanocomposites possess relatively uniform channel-like pores with BJH pore size of about 4 nm. The BET surface area and pore volume of samples are around 170 m^2/g and 0.20 cm^3/g and slightly increase with the increase of HPW content. Mesoporous HPW/TiO_2 shows excellent catalytic activity and selectivity in oxidation of DBT, and DBT conversion enhances with the increase of HPW concentrations. Oxidative reactivity of the model sulfur compounds follows the order of DBT > 4,6-DMDBT > BT. After three times of regeneration, the activity loss of mesoporous HPW/TiO_2 is negligible.

Acknowledgments

This work was financially supported by the Hubei Provincial Department of Education (grant no. Q20081209). Authors wish to thank Mr. Xiaodi Du (Wuhan University of Technology) for his valuable comments and useful discussion.

References

[1] J.T. Sampanthar, H. Xiao, J. Dou, T.Y. Nah, X. Rong, W.P. Kwan, Appl. Catal. B: Environ. 63 (2006) 85.
[2] M. Te, C. Fairbridge, Z. Ring, Appl. Catal. A: Gen. 219 (2001) 267.
[3] G.E. Dolbear, E.R. Skov, Prepr. Am. Chem. Soc. Div. Pet. Chem. 45 (2000) 375.
[4] V. Hulea, F. Fajula, J. Bousquet, J. Catal. 198 (2001) 179.
[5] A.V. Anisimov, E.V. Fedorova, A.Z. Lesnugin, V.M. Senyavin, L.A. Aslanov, V.B. Rybakov, A.V. Tarakanova, Catal. Today 78 (2003) 319.
[6] J. Palomeque, J.M. Clacens, F. Figueras, J. Catal. 211 (2002) 103.
[7] K. Yazu, Y. Yamamoto, T. Furuya, K. Miki, K. Ukegawa, Energy Fuels 15 (2001) 1535.
[8] S. Djangkung, S. Murti, H. Yang, K. Choi, Y. Kora, I. Mochida, Appl. Catal. A: Gen. 252 (2003) 331.
[9] P.S. Tam, J.R. Kittrell, J.W. Eldridge, Ind. Eng. Chem. Res. 29 (1990) 321.
[10] S. Otsuki, T. Nonaka, W. Qian, A. Ishihara, T. Kabe, Bull. Chem. Soc. Jpn. 31 (1998) 1939.
[11] D. Wang, E.W. Qian, H. Amano, K. Okata, A. Ishihara, T. Kabe, Appl. Catal. A 253 (2003) 91.
[12] T.V. Rao, B. Sain, S. Kafola, Y.K. Sharma, S.M. Nanoti, M.O. Garg, Energy Fuels 21 (2007) 3420.
[13] S.Z. Liu, B.H. Wang, B.C. Cui, L.L. Sun, Fuel 87 (2008) 422.
[14] P. De Filippis, M. Scarsella, Ind. Eng. Chem. Res. 47 (2008) 973.
[15] F.M. Collins, A.R. Lucy, C. Sharp, J. Mol. Catal. A: Chem. 117 (1997) 397.
[16] H. Mei, B.W. Mei, T.F. Yen, Fuel 82 (2003) 405.
[17] L.Y. Kong, G. Li, X.S. Wang, Catal. Today 93–95 (2004) 341.
[18] Y. Shiraishi, T. Hirai, I. Komasawa, J. Chem. Eng. Jpn. 35 (2002) 1305.
[19] E. Torres-Garcia, G. Canizal, S. Velumani, L.F. Ramirez-Verduzco, F. Murrieta-Guevara, J.A. Ascencio, Appl. Phys. A 79 (2004) 2037.
[20] Y. Shiraishi, T. Naito, T. Hirai, Ind. Eng. Chem. Res. 42 (2003) 6034.
[21] A.K. Sinha, K. Suzuki, J. Phys. Chem. B 109 (2005) 1708.
[22] M. Kruk, M. Jaroniec, Chem. Mater. 13 (2001) 3169.
[23] B. Yao, L. Zhang, J. Mater. Sci. 34 (1999) 5983.
[24] D. Huang, Y.J. Wang, L.M. Yang, G.S. Luo, Micropor. Mesopor. Mater. 96 (2006) 301.
[25] P.A. Jalil, M.A. Al-Daous, A.A. Al-Arfaj, A.M. Al-Amer, J. Beltramini, S.A.I. Barri, Appl. Catal. A: Gen. 207 (2001) 159.
[26] L.R. Pizzio, P.G. Vázquez, C.V. Cáceres, M.N. Blanco, Appl. Catal. A: Gen. 256 (2003) 125.
[27] Á. Kukovecz, Z. Kónya, I. Kiricsi, J. Mol. Struct. 563–564 (2001) 409.
[28] X. Jiang, T. Herricks, Y. Xia, Adv. Mater. 15 (2003) 1205.
[29] Y. Yang, Q. Wuc, Y. Guoa, C. Hu, J. Mol. Catal. A 225 (2005) 203.
[30] J.G. Yu, M.H. Zhou, B. Cheng, X.J. Zhao, J. Mol. Catal. A: Chem. 246 (2006) 176.
[31] X.D. Yu, Y.N. Guo, L.L. Xu, X. Yang, Y.H. Guo, Colloid Surf. A 316 (2008) 110.
[32] L.C. Caero, E. Hernández, F. Pedraza, F. Murrieta, Catal. Today 107–108 (2005) 564.
[33] A. Ishihara, D.H. Wang, F. Dumeignil, H. Amano, E.W. Qian, T. Kabe, Appl. Catal. A: Gen. 279 (2005) 279.
[34] X.M. Yan, J.H. Lei, D. Liu, Y.C. Wu, W. Liu, Mater. Res. Bull. 42 (2007) 1905.
[35] S.M. Kumbar, G.V. Shanbhag, F. Lefebvre, S.B. Halligudi, J. Mol. Catal. A: Chem. 256 (2006) 324.
[36] L.N. Yang, J. Li, X.D. Yuan, J. Shen, Y.T. Qi, J. Mol. Catal. A: Chem. 262 (2007) 114.